SPECTRUM OF ENGINEERING SCIENCES
ISSN (E) 3007-3138 (P) 3007-312X VOLUME 4, ISSUE 5, 2026

PHOSPHATE RECOVERY FROM EUTROPHIC WATER USING IRON MODIFIED SUGARCANE BAGASSE BIOCHAR: ADSORPTION PERFORMANCE AND FERTILIZER REUSE

Talha Zubair[*1], Muhammad Mudassar Hassan[2], Qaisra Zubair[3], Muhammad Zakriya[4], Syed Kumail Abbas[5]

[*1]*Department of Environmental Technology and Engineering, IHE Delft Institute for Water Education, Delft, Netherlands*
[2]*Institute of Environmental Sciences and Engineering, School of Civil and Environmental Engineering (SCEE), NUST, Islamabad, Pakistan*
[3]*Institute of Environmental Sciences and Engineering, School of Civil and Environmental Engineering (SCEE), NUST, Islamabad, Pakistan*
[4]*Department of Climate Change and Sustainable Development, School of Interdisciplinary Engineering and Sciences (SINES), NUST, Islamabad, Pakistan*
[5]*Institute of Environmental Engineering, Peoples' Friendship University of Russia named after Patrice Lumumba, Moscow, Russia*

[*1]talhazubair2307@gmail.com, [2]hassanmudassar43@gmail.com, [3]qaisrazubair0411@gmail.com, [4]zaakriyakhan@gmail.com, [5]1032249708@pfur.ru

[*1]https://orcid.org/0009-0002-8442-6094, [4]https://orcid.org/0009-0006-3504-1904

DOI:https://doi.org/10.5281/zenodo.20507335

Keywords
iron-modified biochar; sugarcane bagasse; phosphate adsorption; phosphate recovery; pyrolysis; fertilizer reuse; P-loaded biochar fertilizer

Article History
Received: 03 April 2026
Accepted: 15 May 2026
Published: 30 May 2026

Copyright @Author
Corresponding Author: *
Talha Zubair

Abstract
Iron-modified sugarcane bagasse biochar was synthesized and evaluated for phosphate recovery from eutrophic water, as well as its potential reapplication as a phosphate-based soil fertilizer. Biochar dosage, contact time, temperature, pH, and initial phosphate concentration influence the phosphate removal, as shown by batch adsorption experiments. Under acidic conditions, the material achieved 98.5% removal, and under near-neutral conditions at 4 g/L, it achieved 80.3% removal. Iron incorporation was confirmed by SEM-EDS, and after iron modification, changes in pore structure and surface area were observed by BET analysis. According to the equilibrium data, the Langmuir model fitted better than the Freundlich model, and the kinetic data, based on adsorption modelling, followed the pseudo-second-order model, suggesting that phosphate uptake was governed by chemisorption and surface binding. After the application of the Fe-modified phosphate-loaded biochar, the improvement in shoot and root growth was indicated by the preliminary mustard pot test. The results indicated that the iron-modified sugarcane bagasse biochar has the potential for circular phosphate recovery. However, replications of plant growth experiments and actual eutrophic water are needed for validation.

INTRODUCTION

Eutrophication is the excessive release of nutrients, mainly nitrogen and phosphorus, into water bodies, affecting freshwater ecosystems worldwide and causing adverse environmental impacts (Conley et al., 2009; Smith & Schindler, 2009). The main reason for nutrient enrichment, particularly phosphorus (P), is the presence of algae and other aquatic flora. This phenomenon degrades water quality and significantly impacts biodiversity in aquatic ecosystems (Carpenter et al., 1998; Zheng et al., 2019). A variety of sources, including agricultural runoff, wastewater treatment plants, and various anthropogenic activities, contribute to the discharge of phosphorus, further worsening the impacts. Thus, there is a pressing need to devise sustainable, cost-effective strategies to remove nutrients from eutrophic waters (Vikrant et al., 2018; Yang et al., 2018).

In recent years, biochar has emerged as a promising adsorbent, exhibiting significant potential for phosphorus removal from eutrophic water (Vikrant et al., 2018; Luo et al., 2023). Biochar is a carbon-rich substance that is formed through the process of pyrolysis, which involves the thermal decomposition of organic matter (Ahmad et al., 2014; Lehmann & Joseph, 2015). This organic matter can include a variety of waste materials, including municipal solid waste, forestry byproducts, and agricultural residues (Lehmann & Joseph, 2015). Biochar can support phosphate removal, which may help reduce nutrient enrichment (Ahmad et al., 2014; Luo et al., 2023). Furthermore, the process of producing biochar is both economically and environmentally sound and can help sequester carbon, thereby lessening the effects of climate change.

The use of biochar as a phosphate-based fertilizer for plant growth has been limited due to its low solubility and the largely restricted availability of phosphorus, depending on feedstock, pyrolysis temperature, and modifications (Zhao et al., 2016). The inability of biochar to supply soluble phosphorus, which is necessary for optimal plant growth and development, limits its efficacy as a fertilizer (Zheng et al., 2019; Luo et al., 2023). The development of functionalized biochar has therefore attracted increasing attention as a means of improving phosphate recovery, solubility, and fertilizer accessibility. Biochar modified with functional groups such as amino, hydroxyl, and carboxyl groups is referred to as functionalized biochar (Rajapaksha et al., 2016).

Iron activation is one way to functionalize biochar. Iron activation increases the biochar's ability to adsorb phosphorus by activating iron (Fe) into its structure (Luo et al., 2023; Yang et al., 2018). A variety of techniques, such as impregnation with iron salts, pyrolysis in the presence of iron-containing precursors, or incorporating iron-rich materials throughout the biochar formation process, can be used to activate iron (Rajapaksha et al., 2016; Yang et al., 2018). In addition, Iron activation enhances the phosphorus adsorption capacity of biochar, and the P-loaded engineered biochar has been reported to improve seed germination and early seedling growth (Vikrant et al., 2018; Luo et al., 2023).

The significance of this research project lies in its effort to synthesize functionalized biochar via a unique iron-activation process. It will make a significant contribution by developing an economical and environmentally sustainable technique that eliminates the need for harmful substances. The functionalized biochar will exhibit improved phosphorus adsorption capacity and catalytic activity due to the incorporation of iron into its structure. The method mentioned above shows promise for efficiently removing phosphate from eutrophic water and then using the biochar as a phosphate-based fertilizer to improve seed germination and early seedling growth.

The main aim of this study is to synthesize and characterize iron-modified sugarcane bagasse, analyze its phosphate-removal efficiency under different operating conditions, model its adsorption behaviour, and evaluate the potential of using phosphate-loaded biochar as a P-based fertilizer for mustard plant growth.

LITERATURE REVIEW

In research, the literature review is crucial because it lays the groundwork for further investigations. It also facilitates the collection of relevant data, allowing researchers to conduct their studies with

precision and a clear focus. The aforementioned articles were subjected to rigorous inspection to gain a thorough understanding and gather pertinent information for this research.

Because phosphorus (P) contamination negatively impacts ecosystem health and water quality, it is a major concern in aquatic environments (EPA, 2025). This literature review aims to provide a comprehensive overview of current research in the field, with particular emphasis on studies examining phosphate adsorption by modified biochar. This essay summarizes four key studies conducted in this area, emphasizing their key conclusions and the useful implications that follow.

The initial study investigates the adsorption ability of chitosan-modified sugarcane bagasse biochar for inorganic phosphate ions. Manyatshe et al. (2022), in their experimental results, reported that at pH 3 the clearance rate was 40.23%, whereas at pH 8 it was 2.99%. Due to a lack of active sites and the presence of competing pollutants, the researchers found that the removal efficacy was inadequate, even at high pH levels. This finding suggests that chitosan modification may not always improve phosphate adsorption (Manyatshe et al., 2022).

The study of Palansooriya et al. (2021) focused on removing phosphate from water. To achieve this goal, the researchers examined the effectiveness of iron (III)-loaded chitosan biochar fiber-reinforced composites. Several fiber-reinforced composites were found to have maximal adsorption capacities of 9.63, 8.56, 16.43, and 19.24 mg Pg1. The results suggest that adding iron (III) to the chitosan biochar composite may improve its adsorption capacity.

The investigation conducted by Yin et al. (2021) employed computational modelling to examine phosphate adsorption on biochar structures modified with Mg/Ca in aqueous solutions. The findings of their study demonstrated that the biochar structure supplemented with calcium exhibited greater phosphate-absorption efficacy than the biochar structure supplemented with magnesium. Furthermore, the results of the study indicated that metal adsorption was more efficient than edge adsorption, highlighting the importance of the modified metal within the biochar framework for H2PO4 adsorption. The aforementioned findings elucidate the underlying mechanisms of phosphate adsorption on engineered biochar (Yin et al., 2021).

Choi et al. (2018) analyzed the sequestration of phosphorus in water through the utilization of an innovative biochar derived from dairy manure coated with calcium hydroxide. The $Ca(OH)_2$-BC exhibited a maximum removal efficiency of 89%, accompanied by an adsorption capacity of 13.6 mg/g. The biochar coated with calcium hydroxide exhibited superior performance compared to biochar treated with calcium oxide and magnesium oxide. However, the performance of biochar was found to be inferior to that of FeO and ZnO. The results of this study indicate that calcium hydroxide-treated biochar is highly effective at removing phosphate from the surrounding ecosystem (Zhang et al., 2021).

Taken as a whole, the articles reviewed provide substantial data on how to create and characterize modified biochar materials for phosphate removal. While potential improvements in phosphate adsorption capacity were observed when Iron Oxide and calcium were included, limitations in pH-dependent phosphate removal were observed for chitosan-modified biochar. Calcium hydroxide-coated biochar, unlike other coated biochar materials, has been shown to be an effective adsorbent with enhanced adsorption capacity. These findings provide light on the mechanism of phosphate removal and will inform the development of more efficient and long-lasting techniques for removing phosphate from aqueous solutions in the future (Zhang et al., 2021).

METHODOLOGY

The following methodology was employed to achieve the objectives of this research project.

3.1 Sugarcane Bagasse Pre-processing

3.1.1 Acquisition of Primary Resources

The sugarcane bagasse was generated by a sugar mill and subsequently transported to a laboratory for processing.

3.1.2 Sorting and Cleaning

A comprehensive analysis was conducted on the collected bagasse to remove any undesirable substances, including stones, plastics, and metals. Subsequently, a washing procedure was conducted with distilled water to remove particulate matter, such as dirt and dust.

3.1.3 Desiccation

The bagasse was subjected to thermal treatment and kept in the oven at 105°C for 24 hours until it reached a stable weight. The objective of the procedure was to remove moisture from the bagasse, as it could affect subsequent stages of processing.

3.1.4 Process of Grinding

Using the laboratory grinder, the desiccated bagasse was pulverized into fine particles to a specified size.

3.1.5 The Process of Sieving

It is also known as screening and is a method for separating particles of different sizes by passing them through a sieve. The pulverized sugarcane bagasse was sieved using a 0.2 mm mesh to remove larger particles and achieve a consistent particle size distribution.

3.1.6 Chemical Treatment

It refers to the application of chemical substances in order to modify or alter the properties of a material or substance.

The bagasse underwent a treatment with alcohol at a specific concentration. The primary objective of this procedure was to eliminate all impurities and enhance the purity of the bagasse.

3.1.7 Cleansing

After the treatment procedure was complete, it was rinsed thoroughly with distilled water to remove any residual chemicals.

3.1.8 Drying Process

The cleaned bagasse was dried at 500 degrees Celsius at a rate of 16 degrees per minute until a constant weight was achieved. The bagasse dried out some of the moisture remaining after the chemical treatment.

3.1.9 The Storing Procedure

Containers were used to keep the processed bagasse at room temperature until it could be used. After undergoing the aforementioned steps, the sugarcane bagasse was ready for use in experiments and analyses.

3.2 Pyrolysis Process

The pyrolysis process of sugarcane bagasse will be discussed in this section.

3.2.1 Introduction to the Pyrolysis Reactor Loading Process

The bagasse was introduced into the pyrolysis reactor in powdered form. The reactor was designed to operate within a 500°C temperature range while maintaining a heating rate of 16°C per minute.

3.2.2 Purging

To mitigate the risk of substrate oxidation, nitrogen gas (N2) was used to purge the reactor in order to remove any traces of air and eliminate the possibility of air contamination.

3.2.3 Pyrolysis Process

With a heating rate of 16°C per minute, the reactor was heated to the specified temperature of 500°C. The feedstock was converted into biochar, bio-oil, and biogas.

3.2.4 Thermal Dissipation

Following completion of the above procedure, the reactor was cooled to ambient temperature while shielded in a nitrogen atmosphere.

3.2.5 Product Collection

For later use, the biochar, bio-oil, and synthetic gas produced by the pyrolysis process were collected separately and stored in sealed containers.

Sugarcane bagasse was pyrolyzed under controlled conditions after the previously indicated procedures, and the resulting material was subsequently used for analytical and experimental purposes.

3.3 Criteria for Pyrolysis Reactor

The biochar synthesis technique comprises the following conditions:

- The synthesis is conducted at a temperature of 500 degrees Celsius.
- The heating rate employed in this study involves a rapid temperature increase of 16°C per minute.

The N2 purging rates at various stages of the process were examined:

- The introduction of nitrogen gas (N_2) into the reactor occurs at a flow rate of 0.2 liters per minute, and the purging process typically lasts 10 to 15 minutes.
- A constant flow of nitrogen gas (N_2) is kept constant at 0.1 liter/min for the duration of the process (three hours).
- Following the pyrolysis process, a purging of N_2 gas is conducted at a rate of 0.5 liters per minute for a duration of 15-20 minutes.

Figure 1

Pyrolysis Reactor

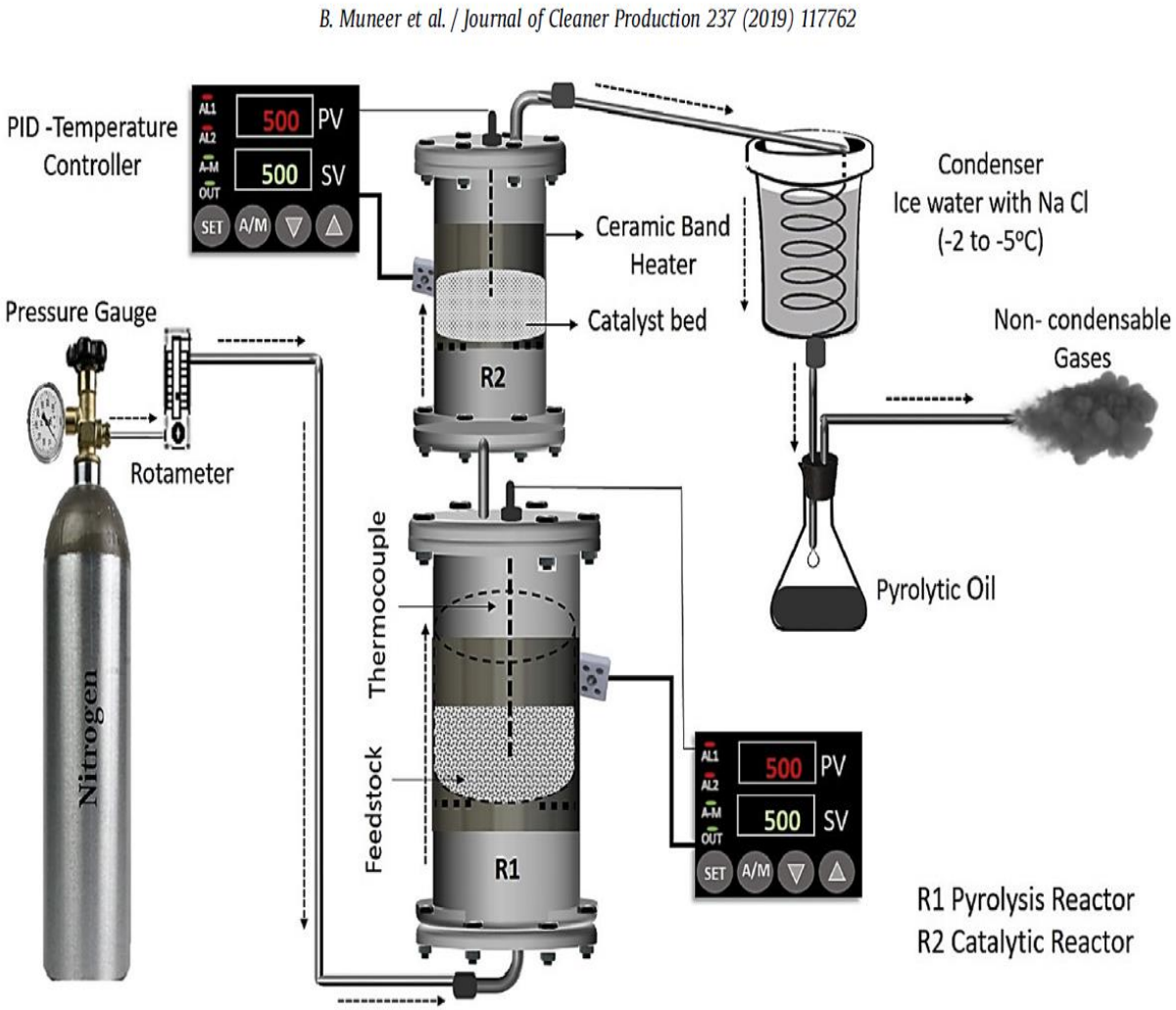

3.4 Investigation into the pyrolysis byproducts

3.4.1 Initial Execution

One hundred grams of biomass was used in the first experiment, yielding the following amounts of pyrolysis products:

- The quantity of bio-oil under consideration is 38.3 grams.
- The quantity of biochar utilized in the experiment was 49.7 grams.
- The quantity of biogas produced is 12 g.

3.4.2 Second Iteration

A total of 43.6 grams of biomass was added to the reactor in the succeeding experimental session, yielding the aforementioned amounts of pyrolysis products.

- The quantity of bio-oil under consideration is 15.4 grams.
- The quantity of biochar utilized in the experiment was 21.7 grams.
- The biogas sample yielded a mass of 6.5 grams.

Compared to bio-oil, a liquid product, and biogas, a gaseous product, the pyrolysis method produced a greater proportion of biochar, a solid residue. During the initial trial, it was observed that 49.77% of the initial biomass underwent a transformation process resulting in the formation of biochar, while 35.3% was converted into bio-oil, and the remaining 14.9% was transformed into biogas. During the second iteration, approximately 49.8% of the biomass underwent a transformation process resulting in the formation of biochar, while 35.4% of the biomass was converted into bio-oil. Additionally, 14.9% of the biomass was transformed into biogas.

3.5 Iron Activation

Biochar (10 grams) was added to a 0.1 molar $FeCl_3.6H_2O$ solution. By adding 0.5M NaOH solution, the pH of the solution was adjusted to 11. The solution was heated on a hot plate agitator for 45 minutes at a temperature of 60°C. Following the cooling procedure, the solution was filtered, and the pH was neutralized to 7 by adding distilled water. The stable biochar residue was then separated from the liquid by centrifuging the solution.

3.6 Methodology for P-detection

To execute the procedure, we added 2.5 grams of Ammonium Molybdate into 30 milliliters of distilled water, followed by 0.125 grams of Ammonium Metavanadate to an additional 30 milliliters of distilled water. The Ammonium Metavanadate solution was heated and then cooled. After this, 33 mL of hydrochloric acid (HCl) was added to the Ammonium Metavanadate-containing solution, and the solution was then cooled again. The Ammonium Molybdate solution was added to the mixture of Ammonium Metavanadate and hydrochloric acid (HCl) to reach a final volume of 100 mL. Using the stock solution and the reagents, a calibration curve was finally acquired. Researchers of this present study have shown a linear relationship between absorbance and phosphate content using the calibration curve.

Ammonium molybdate and ammonium metavanadate were used in an effective and proven method for detecting phosphate. The proposed approach may find use in a wide variety of contexts, such as environmental monitoring and agricultural activities.

3.7 Characterization

3.7.1 Prior to Activation

3.7.1.1 The Scanning Electron Microscopy-Energy Dispersive X-ray Spectroscopy (SEM-EDS) technique. This method is used to investigate the material's surface morphology or microstructure to determine its elemental composition.

3.7.1.2 The BET Analysis Method. It is a widely used technique in surface chemistry and materials science. The BET analysis method is employed to quantify the material's specific surface area, porosity, pore size, and pore volume. This provides details on the material's texture and surface properties.

3.7.1.3 The Proximate Procedure. The chemical composition of a substance, by measuring its various components such as moisture, ash, protein, fat, and carbohydrates, can be found by this method.

3.7.2 Following the Activation Process

3.7.2.1 SEM-EDS. Using SEM-EDS, the surface morphology and elemental composition of the material following activation are examined in a manner analogous to its condition prior to activation. It facilitates the evaluation of any structural modifications to the material.

3.7.2.2 Brunauer-Emmett-Teller (BET) Analysis. It measures the surface area, porosity, pore size, and pore volume of the activated material. This facilitates the evaluation of the change in its surface characteristics and permeability.

3.7.2.3 Proximate Procedure. It refers to an analytical technique for determining a substance's composition by examining its components, such as moisture content and ash.

3.8 Batch Experiments

Various batch experiments were conducted in order to observe and evaluate the effects of the following significant variables.

3.8.1 Biochar Dosage

Biochar dosage was varied to check the optimal dosage. The biochar dosage utilized in the experimental study was taken first 0.1grams. A subsequent experiment was conducted using 0.2 grams of biochar. Another adsorption experiment in which 0.5 g of biochar was used. Then, 1gram of biochar was used in the subsequent experimental procedure. The experiment was run again, this time with twice as much biochar (2 grams). Similarly, 3 g of biochar was used in an adsorption experiment. After this, four grams of biochar were utilized. In the final trial of the adsorption test, a biochar dosage of 5 grams was used, and the results were obtained.

3.8.2 Initial Phosphate Concentration

PO_4-P concentration was varied to check the optimal initial concentration. Initially, the PO4-P concentration was specified at 5 milligrams per liter. Secondly, 10 milligrams per liter PO_4-P was taken. Then the concentration was adjusted to 12 milligrams per liter. Similarly, 15 mg/L PO_4-P was used. Following the same procedure, we then conducted the experiment at 18 milligrams per liter. Finally, 20 milligrams per liter were utilized, and the results were obtained.

3.8.3 pH

The experimental study investigated the effect of pH levels (2, 5, 7, and 9) on the adsorption capacity and removal efficiency of biochar.

3.8.4 Contact Period

To see how changing contact time affected the adsorption process, we conducted an experiment. We studied time periods of 6mins, 12mins, 30mins, 60mins, and 240mins of interaction. Adsorbate and adsorbent may interact more deeply if given more time during the contact phase. Increases in contact time result in a linear rise in adsorption capacity.

The investigation found that the absorption capacity improved as the contact time went from 0.1 to 4 hours. Nonetheless, it is possible that there exists a threshold beyond which the adsorption capacity does not increase appreciably despite prolonged contact times.

It was observed that the contact time between the compounds significantly influenced the adsorption capacity. The extended contact periods typically result in enhanced adsorption capacities.

3.8.5 Temperature

The temperature measured was 25 degrees Celsius. At 35°C, a further experiment was conducted. In the succeeding test, the temperature increased to 45 degrees Celsius.

The experimental investigation consisted of using 500 mL conical flasks, each containing 100 mL of phosphate solution prepared from the initial stock solution. Either NaOH or HCl was used to adjust the solution's pH. The specimen was treated with varying concentrations of biochar. After attaining the desired temperature, the flask was shaken at a constant rate of 200 revolutions per minute (rpm) using a shaker. Phosphate content was measured by taking samples at regular intervals and analyzing them using a UV-Vis spectrophotometer set to a wavelength of 470nm.

3.8.6 Soil Collection and Preparation

To carry out this step, we procured soil samples from the NUST nursery near Gate 2. These soil samples were subjected to a series of processes to ensure the conditions for the pot test experiment.

3.8.6.1 Desiccation. The collected soil samples were dried in an oven at 105°C to remove all traces of moisture. This dehydration process was of great importance, as it provided accurate measurements and prevented the visible growth of microorganisms during the experiment.

3.8.6.2 Pulverization. Once the soil samples had undergone the important dehydration process, they were then rammed and ground with a mortar and pestle. This pulverisation technique resulted in homogeneous particle size and promoted adsorption with the biochar.

3.8.6.3 Sieving. After removing contaminants, the pulverized soil was sieved through a 2mm mesh sieve to remove larger particles and ensure a uniform distribution. This procedure produced a uniform soil mixture suitable for the pot test.

3.8.6.4 Pot Test Arrangement. As an initial observation, this pot test was conducted. Furthermore, it was not developed as a replicable statistical agronomic trial. Biochar and soil were well combined in the pot test at a 2% biochar-to-98 % soil ratio. In particular, 49 grams of soil and 1 gram of biochar were combined. The mustard plant seed (Brassica juncea) was used for this experiment.

3.8.6.5 Root and Shoot Length Observations. After preparing the hallowed pot test setup, the mustard plant was planted in the soil-biochar mixture under controlled conditions. Throughout its growth cycle, the lengths of both its roots and shoots were carefully measured at regular intervals, capturing the whole progression (Vikrant et al., 2018).

RESULTS AND DISCUSSION

4.1 Batch Adsorption Experiments

4.1.1 Biochar Dosage

With increasing biochar dosage, phosphate removal efficiency also increases, reaching 80.3% at 4 g/L. However, the 5 g/L dosage yielded a slightly higher phosphate removal efficiency of about 81.1%, while the adsorption capacity decreased sharply to 1.6 mg/g, making the 4 g/L biochar dosage the more appropriate operating dose.

Table 1

Effect of Biochar Dosages on the Removal Performance and Adsorption Capacity of Iron-functionalized Biochar Towards Phosphate from Water

Bio-char Dosage (g/L)	Removal Efficiency (%)	Adsorption Capacity (mg/g)
0.1	9.4	9.4
0.2	18.6	9.3
0.5	31.1	6.2
1	52.8	5.2
2	63.6	3.2
3	73.6	2.5
4	80.3	4.5
5	81.1	1.6

4.1.2 pH

The adsorption capacity decreases as the pH rises; the maximum adsorption capacity is observed at acidic pH, which performed the best for both adsorption capacity and removal efficacy. At a pH of 2, a maximum removal efficacy of 98.5% could

be attained. This phenomenon can be attributed to electrostatic interactions between the biochar's surface charge and phosphate ions. Phosphates exhibit an affinity for biochar within an acidic environment, owing to the activation of biochar facilitated by iron and its inherent positive charge. Therefore, the presence of acidity creates a favorable environment for adsorption.

Table 2

Effect of pH on the Removal Performance and Adsorption Capacity of Iron-functionalized Biochar Towards Phosphate from Water

pH	Removal Efficiency (%)	Adsorption Capacity (mg/g)
2	98.5	2.6
5	91.1	2.3
7	80.3	2
9	67.7	1.7

Although phosphate removal was achieved at a maximum pH of 2, in actual treatment of eutrophic water, this condition is less practical due to increased chemical costs, the pH-adjustment requirements of widespread acidification, and the potential to introduce ecological risks before discharge. So, the pH near-neutral range is more applicable and relevant for such an application. Findings indicated that at pH 7, 80.3% phosphate removal was achieved, showing that the biochar remained effective under more realistic water-treatment conditions.

4.1.3 Contact Tim

The maximum removal efficacy was observed as the contact time increased to 4 hours. However, the outcomes obtained at 2 hours and 4 hours exhibited similar trends. Therefore, the optimal duration for contact was determined to be 2 hours. The occurrence in question arises from the equilibrium state of adsorption, in which the rate of adsorption equals the rate of desorption.

Table 3

Effect of Contact Time on the Removal Performance and Adsorption Capacity of Iron-functionalized Biochar Towards Phosphate from Water

Contact Time (HRS)	Removal Efficiency (%)	Adsorption Capacity (mg/g)
0.1	42.7	1.1
0.2	51.8	1.3
0.5	59.5	1.5
1	68.6	1.7
2	80.3	2
4	84.2	2.1

4.1.4 Phosphates Initial Concentration

The increase in the initial phosphate concentration in the solution resulted in a corresponding increase in adsorption capacity. The phenomenon arises from the saturation of adsorption sites on the biochar surface when initial concentrations increase. Conversely, a removal efficiency of 80.25% was observed at an initial phosphate concentration of 5 mg/L. 10 mg/L was chosen as the optimal initial phosphate concentration.

Table 4

Effect of PO4-P Concentration on the Removal Performance and Adsorption Capacity of Iron-functionalized Biochar Towards Phosphate from Water

PO4-P Concentration (mg/l)	Removal Efficiency (%)	Adsorption Capacity (mg/g)
5	83.2	1.1
10	80.3	2
12	75.8	2.3
15	67.8	2.5
18	62.4	2.8
20	54.4	2

4.1.5 Temperature

Temperature generally influences the adsorption process, and temperature changes can affect adsorption capacity. In our experimental investigation, we observed that as the temperature rose to 35°C, the adsorption rate decreased. The effect of ambient temperature on the adsorption rate clarifies this phenomenon.

At lower temperatures, particle motion becomes constrained, resulting in relatively low kinetic energy. The deceleration of adsorbate molecules and their subsequent interaction with the adsorbent surface are impeded by this phenomenon. Consequently, the rate of adsorption decelerates, leading to a diminished adsorption capacity.

Nevertheless, as the temperature rises, the kinetic energy of the molecules increases. This increased energy enhances the adaptability of the adsorption material molecules, allowing them to overcome intermolecular interactions and attach to the adsorbent's surface more readily. As a result, at higher temperatures, the rate of adsorption increases, leading to greater adsorption capacity.

The phenomenon can be attributed to very high thermal energy, which leads to desorption or weakened interactions between the adsorbent and adsorbate. During the course of the study's investigation, the researchers observed a decline in adsorption capacity beyond a temperature threshold of 35 degrees Celsius.

Figure 2

Effect of Temperature on the Removal Performance of Iron-loaded Biochar Towards Phosphate Water

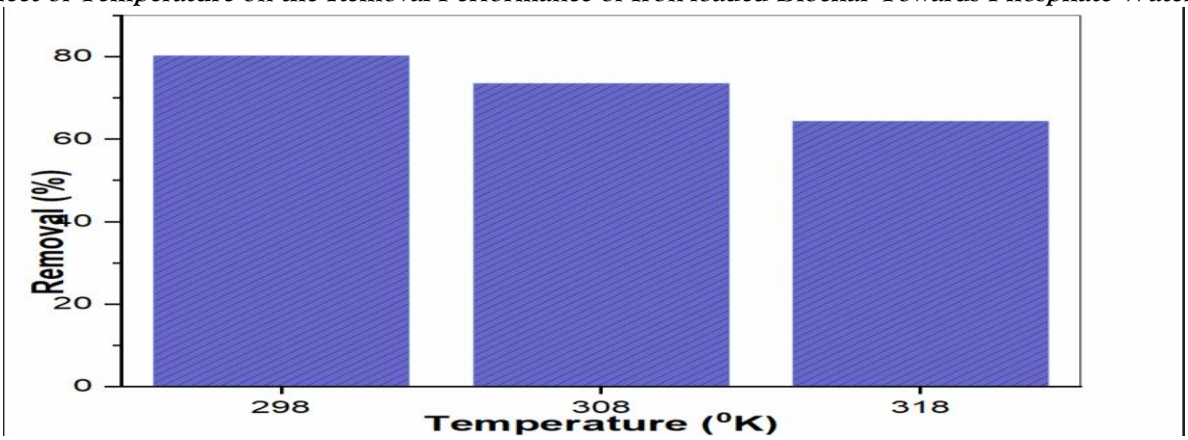

4.2 SEM-EDS

4.2.1 For Raw Biochar

Figure 3

SEM of Raw Biochar x1000

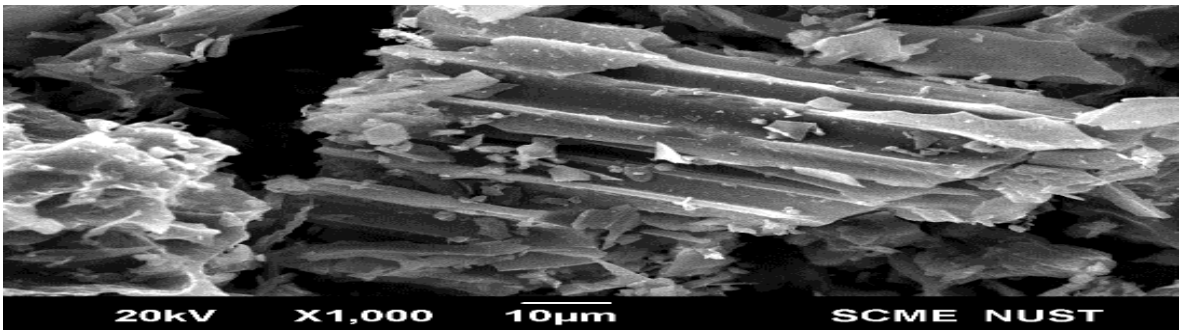

Figure 4
EDS of Raw Biochar Tabular Form

eZAF Quant Result - Analysis Uncertainty: 14.48 %

Element	Weight %	MDL	Atomic %	Error %
C K	77.1	1.02	85.9	10.0
O K	13.0	0.30	10.9	12.6
Mg K	0.8	0.09	0.5	10.8
P K	3.0	0.08	1.3	3.7
K K	1.4	0.10	0.5	5.3
Cu K	2.5	0.29	0.5	9.0
Zn K	2.2	0.35	0.4	4.8

4.2.2 Iron-Biochar
Figure 5
SEM of Fe Bio char x1000

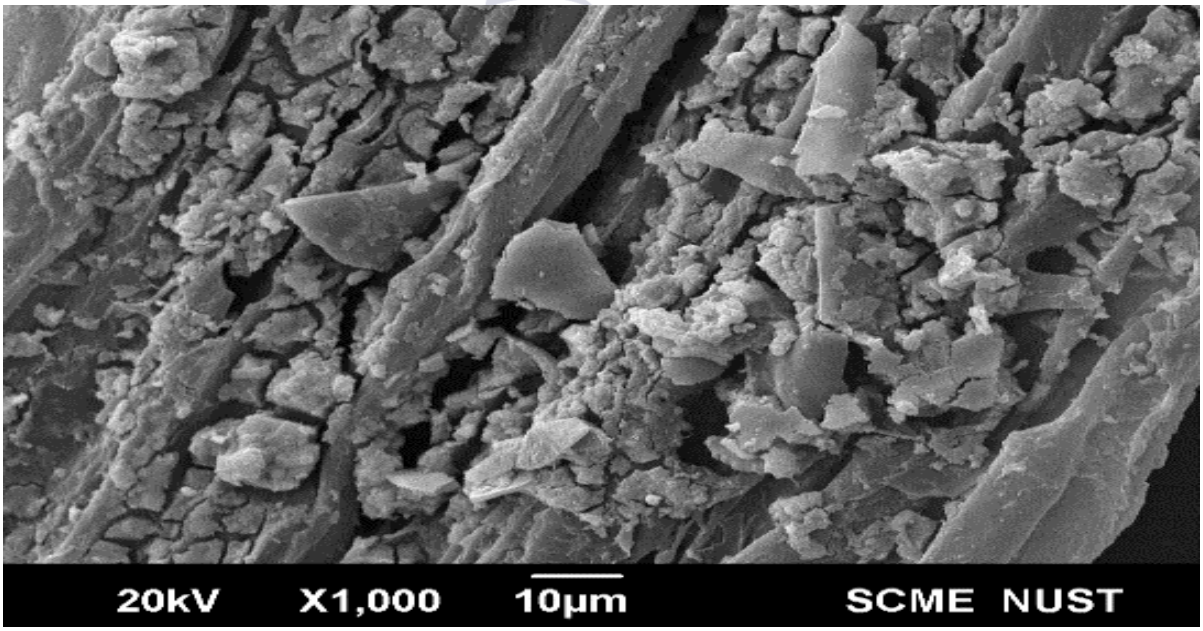

The results above are SEM images in pictorial form, employing a specific lens and precision: 10 µm resolution at 1000X magnification for Raw Biochar and Iron-Loaded Biochar. SEM analysis indicated that raw biochar and iron-modified biochar exhibited irregular, porous, and rough

surface morphologies. The surface of raw biochar seemed more fibrous in contrast to the iron-modified biochar, which indicated textural changes and surface deposits after iron treatment.

Figure 6

EDS of Iron-Biochar Tabular Form

eZAF Quant Result – Analysis Uncertainty: 11.29 %

Element	Weight %	MDL	Atomic %	Error %
C K	40.7	1.32	59.7	11.0
O K	27.6	0.37	30.4	10.8
K K	0.4	0.13	0.2	18.0
Fe K	27.4	0.28	8.6	2.5
Cu K	2.2	0.42	0.6	16.7
Zn K	1.6	0.50	0.4	6.6

EDS (Energy-Dispersive X-ray Spectroscopy) analysis indicated that carbon and oxygen were the primary constituents of the raw biochar, as expected, because sugarcane bagasse is a carbon-rich biomass feedstock. After iron modification, the EDS spectrum of the modified biochar indicates that iron was successfully loaded onto the biochar surface. However, SEM-EDS can only validate surface morphology and elemental existence; it cannot determine the precise chemical bonding environment of iron on biochar. As a result, the Fe-biochar modification should be classified as iron loading or surface incorporation rather than proven chemical bonding.

IEER
Institute for Excellence in Education & Research

4.3 BET Analysis

Table 5

Surface Properties of Raw Biochar and Iron-Biochar

Characteristics	Raw Biochar	Iron-Biochar
Pore volume (cm^3/g)	0.05	1
Pore diameter (nm)	1.7	1.2
Surface area (m^2/g)	31.6	27.2

Sugarcane bagasse biochar exhibits a narrowing of the pore-size distribution throughout the activation process. The addition of iron to the outer layer of raw sugarcane bagasse may account for the observed reduction in surface area and pore volume. It is possible that the introduction of iron injection has resulted in the formation of pore blockages within the biochar.

During activation, it is possible to introduce substances such as iron to modify the characteristics of the biochar. In this scenario, the presence of iron on the surface of raw sugarcane bagasse (RBC) may have obstructed pores, thereby impeding the internal pore structure.

Consequently, the surface area available for adsorption decreases. The dimensions and capacity of the pores, which serve as indicators of their size and volume, are reduced due to the effects caused by the presence of iron.

4.4 Proximate Analysis

Table 6

Properties of Raw Biochar and Iron-Biochar

	Moisture Content	Volatile Combustible Matter	Fixed Carbon	Ash Content
Raw SBC	12.7 %	67.9 %	16.1 %	3.3%
Raw Biochar	7.6 %	49.4 %	40 %	3 %
Fe-Biochar	11.6 %	32.8 %	53.6 %	2 %

The data presented in the table indicates a decrease in volatile combustible matter after the activation, which is resulting in an increase in fixed carbon content.

4.5 Modelling of Isotherm Data

Table 7

Isotherm Data of the Freundlich and Langmuir Models

Model	Equation	Plot	K_f	N	R-Square
Freundlich	$Q_e = k.C^{1/n}$	Q_e	1.5	3.3	0.956
Langmuir	$Q_e = (q_m.k.C_e) / (1+(k.C_e))$	Q_e	3.2	0.8	0.993

Figure 7

Graphical representation of Isotherm Data

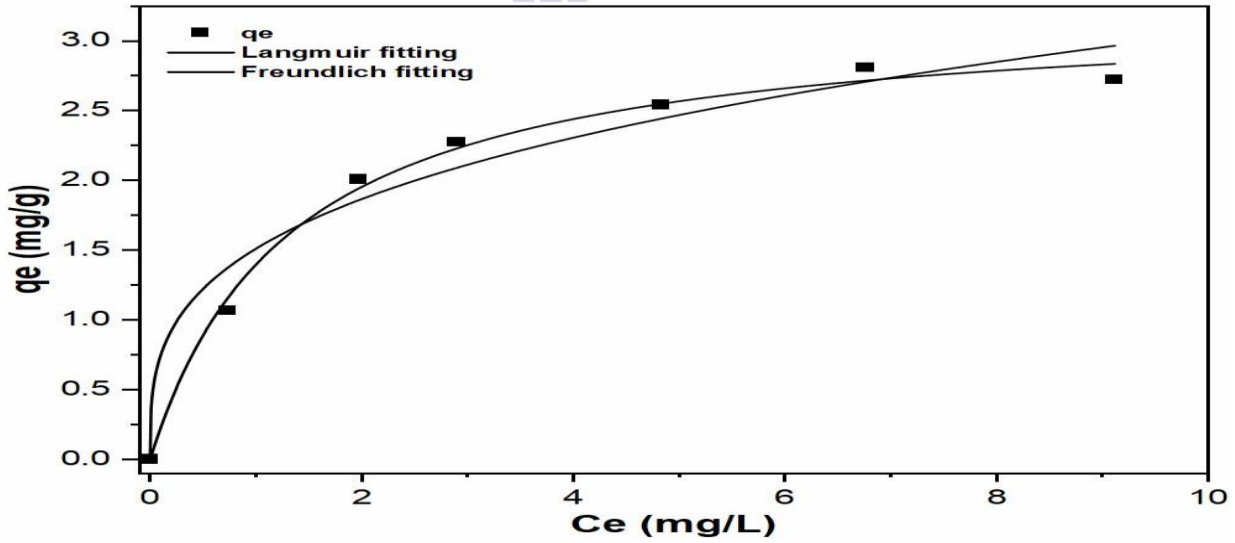

The adsorption mechanism of biochar is demonstrated using isotherm models. The present observation presents two distinct mathematical models, namely the Langmuir and Freundlich curves, which exhibit numerous characteristics. Nevertheless, this biochar product exhibits a strong affinity for Langmuir curve fitting, revealing its impressive capabilities for monolayer adsorption. As a result, this process enhances the exceptional adsorption capacity of biochar, enabling it to effectively capture phosphate ions in its active sites.

As indicated by the higher R^2 value, the Langmuir model fitted the data better than the Freundlich model, suggesting that phosphate adsorption primarily occurred via monolayer coverage of the available active sites on iron-modified biochar.

4.6 Modelling of Kinetic Data

Table 8

Kinetic Data of Pseudo First Order (PFO) and Pseudo Second Order (PSO)

Model	Equation	Plot	Q_e	K_t	R-Square
PFO	$Q_t = q_e - (\exp((\ln(q_e)) - (k.t)))$	Q_t	1.9	2.6	0.9147
PSO	$Q_t = ((k.q_e^2.t) / (1 + (k.q_e.t)))$	Q_t	2.2	1.6	0.9573

Figure 8

Graphical Representation of Kinetic Data

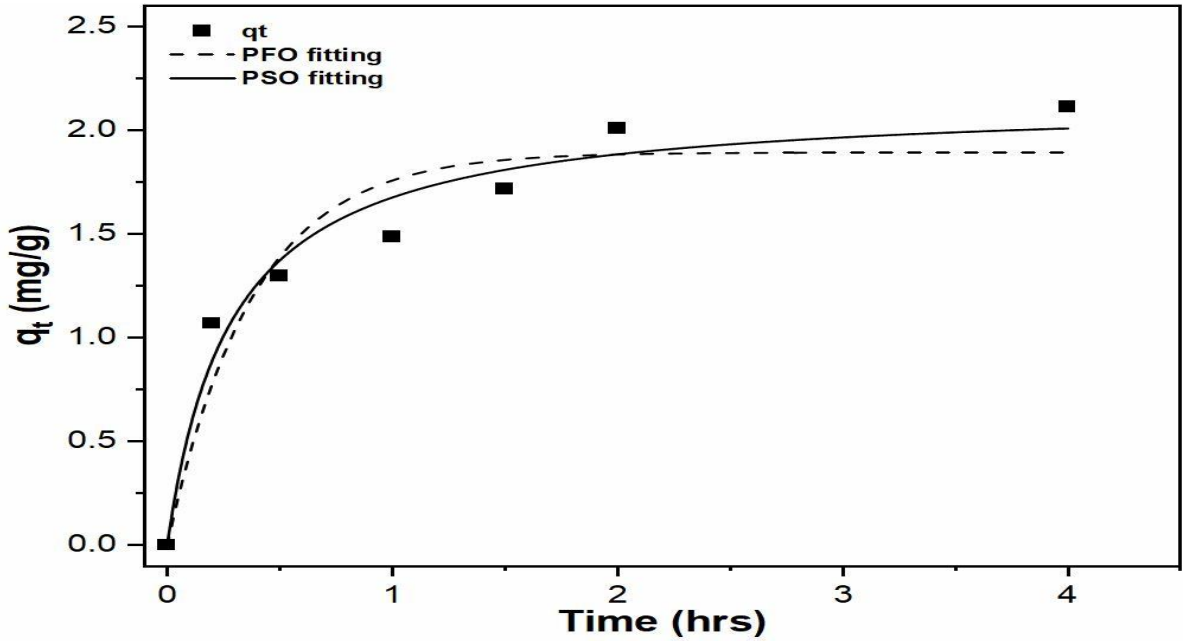

Based on the dynamic data shown in Table 10, it is apparent that the adsorption of the adsorbate onto the iron-activated biochar follows the Pseudo-Second-Order (PSO) model. The PSO framework provides a more precise depiction of the adsorption kinetics for this system than the Pseudo-First-Order (PFO) model, as shown in Table 8.

The PSO model equation is as follows:

$Qt = (k.q_e^2.t) / (1 + (k.q_e.t))$

Wherein, Qt represents the quantity of adsorbate assimilated at time t (mg/g), K denotes the constant of the PSO model (g/(mg·min)), Q_e stands for the equilibrium adsorption capacity (mg/g), and T symbolizes the contact time (min).

From Table 8, the values of q_e and k for the PSO model are observed as 2.2 and 1.6, respectively. These values represent the equilibrium adsorption capacity and the constant K for the PSO model. Besides, an adjusted R-squared value of 0.9 signifies a commendable fit of the PSO model to the empirical data.

The PSO model suggests that the rate-controlling step in adsorption on iron-activated biochar involves a chemical interaction between the adsorbate and sites on the biochar surface. It is worth noting that the PSO model treats the interaction between the adsorbate and the biochar surface as a chemisorption process, consistent with the prevailing activated iron species on the biochar surface.

The PSO model equation shows a distinctive pattern in the graph of qt (amount of adsorbate assimilated at time t) against time, as shown in the table. Fitting empirical adsorption data on Fe-activated biochar to this equation provides insights into adsorption kinetics and helps determine kinetic parameters.

Overall, the observation that adsorption of the adsorbate onto iron-activated biochar follows the Pseudo-Second-Order model implies that chemisorption involving activated iron species on the biochar surface plays a pivotal role in the adsorption mechanism. This discovery has significant implications for optimizing the efficacy of iron-activated biochar as an adsorbent across a wide range of water and wastewater treatment applications, where efficient contaminant removal is highly desired.

4.7 Proposed Phosphate Adsorption Mechanism

The improved phosphate removal by iron-modified sugarcane bagasse biochar can be linked to the incorporation of iron-containing active sites on its surface. SEM-EDS confirmed the presence of iron after modification, while BET analysis revealed changes in surface characteristics after activation. Phosphate uptake was most likely the result of electrostatic attraction under acidic conditions, ligand exchange between phosphate species and surface hydroxyl groups, and inner-sphere complexation with iron sites. The kinetic modelling analysis showed that the pseudo-second-order kinetic model provided the better fit, supporting the significance of chemical interactions in phosphate adsorption. Nevertheless, because advanced surface analyses such as XPS (X-ray photoelectron spectroscopy) were not performed, the mechanism must be demonstrated as proposed rather than indisputably established.

4.8 Gibbs Free Energy

The Gibbs free energy provides crucial insights into the feasibility of our adsorbent activity in the context of our adsorption process. We carried out an adsorption experiment that generated positive outcomes by seeking an exothermic reaction.

Diverse intermolecular forces modify the affinity of the adsorbate and adsorbent. We can determine the thermodynamic favorability of the adsorption approach by computing the Gibbs free energy change (G).

The researchers' laboratory experiments in the present study led them to use the formula G = H - TS. The following are necessary for evaluating the iron-loaded biochar (Fe-BC) adsorption study's data: The slope of the line (b) is 0.10645, indicating a positive connection between adsorption capacity (Y) and adsorbate concentration (x), and the computed value for the intersection of lines (a) is -31.7903.

The data fit the regression model well, as indicated by the adjusted R-squared of 0.90177. This indicates that the adsorption onto the Fe-BC surface is dose-dependent. Ultimately, the results of this study suggest that the researchers' adsorption method used in this study has thermodynamic benefits, as the process was exothermic and a clear association was observed between adsorption capacity and adsorbate concentration. The Gibbs free energy (G) and the total energy of the system were both reduced following adsorption due to the high affinity the adsorbate molecules showed for the Fe-BC surface. According to the thermodynamic analysis, phosphate adsorption was temperature-sensitive. Nonetheless, further verification of thermodynamic parameters and equilibrium constants is needed before claiming exothermicity and spontaneity.

Table 9

Gibbs free energy

Plot		Intercept		R-Square
Equation	**Weight**		**Slope**	
	Fe-BC		-31.8	0.9924
$\Delta G = \Delta H - T\Delta S$	No Weighting		0.1	

Figure 9
Graphical Representation of Gibbs Free Energy

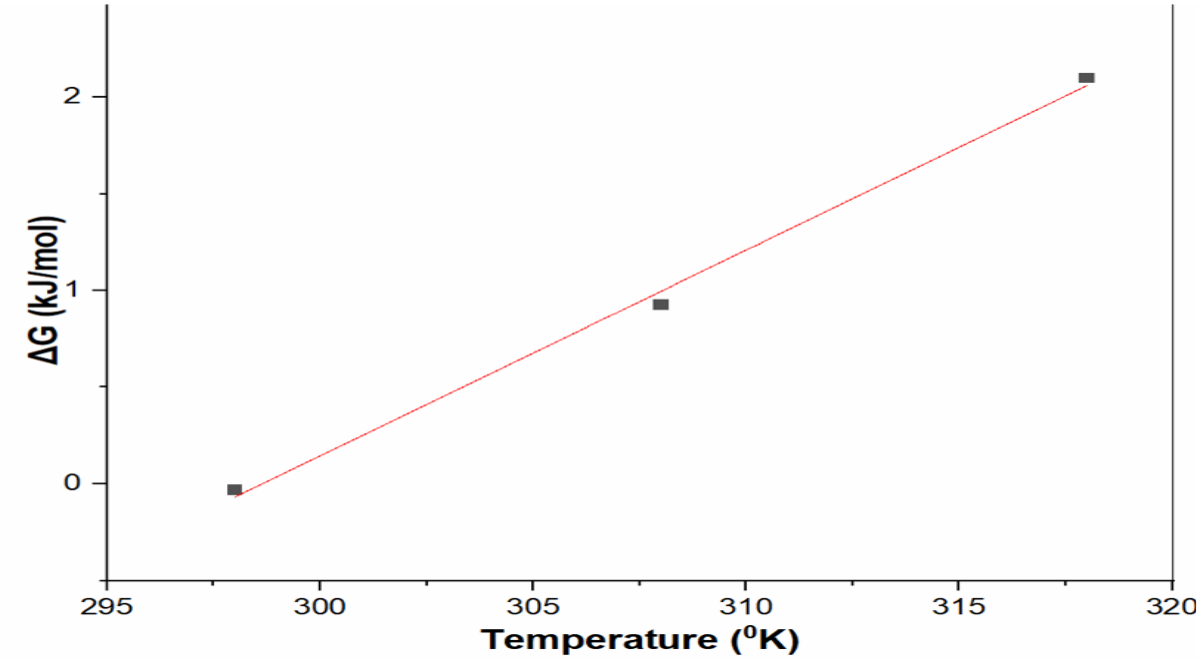

4.8 Pot Test (Phosphate-based Fertilizer)
Figure 10
Pictorial Representation of Pot Test

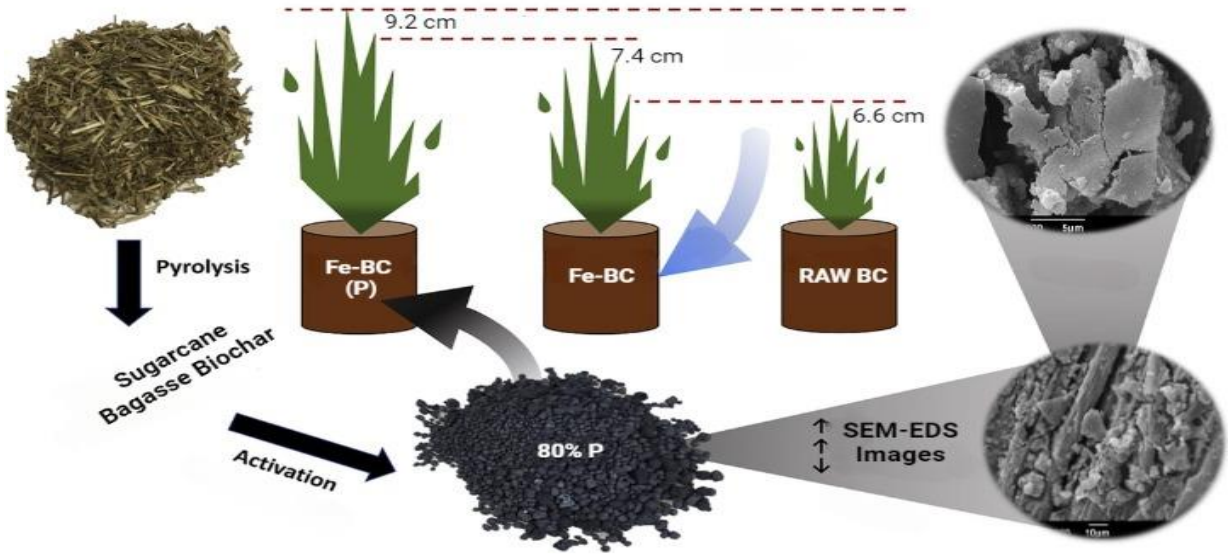

Figure 11
Comparison of Root Length of Plant Before and After Activation of Biochar with Iron

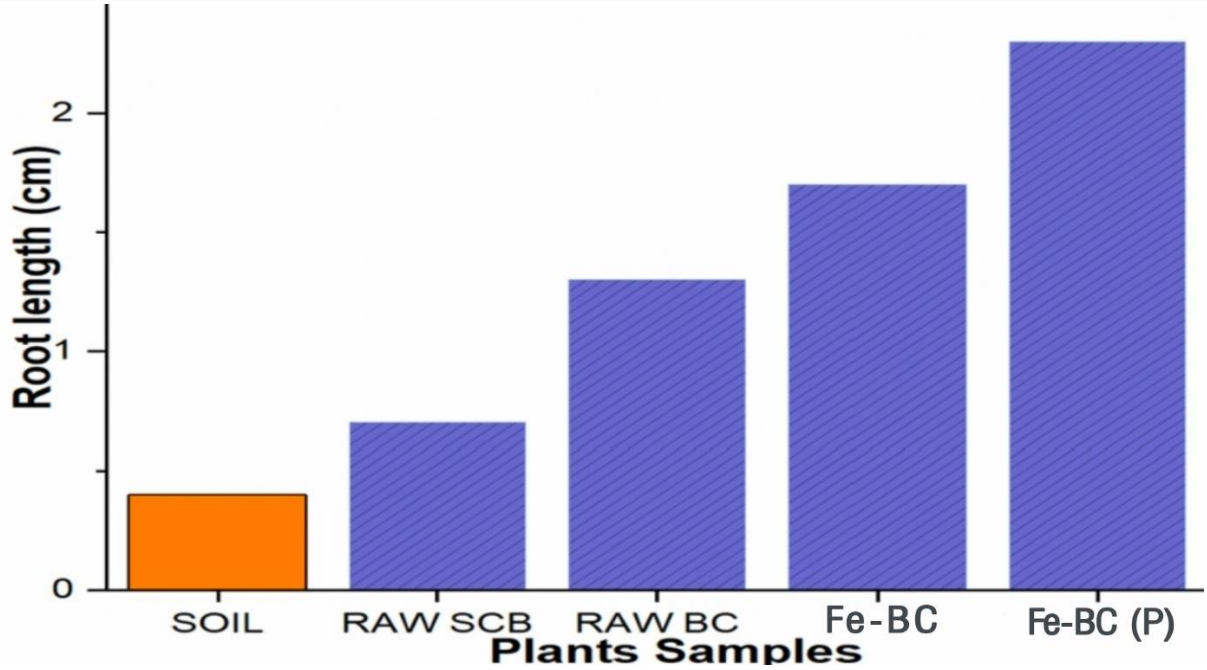

Figure 12

Comparison of Shoot Length of Plant Before and After Activation of Biochar with Iron

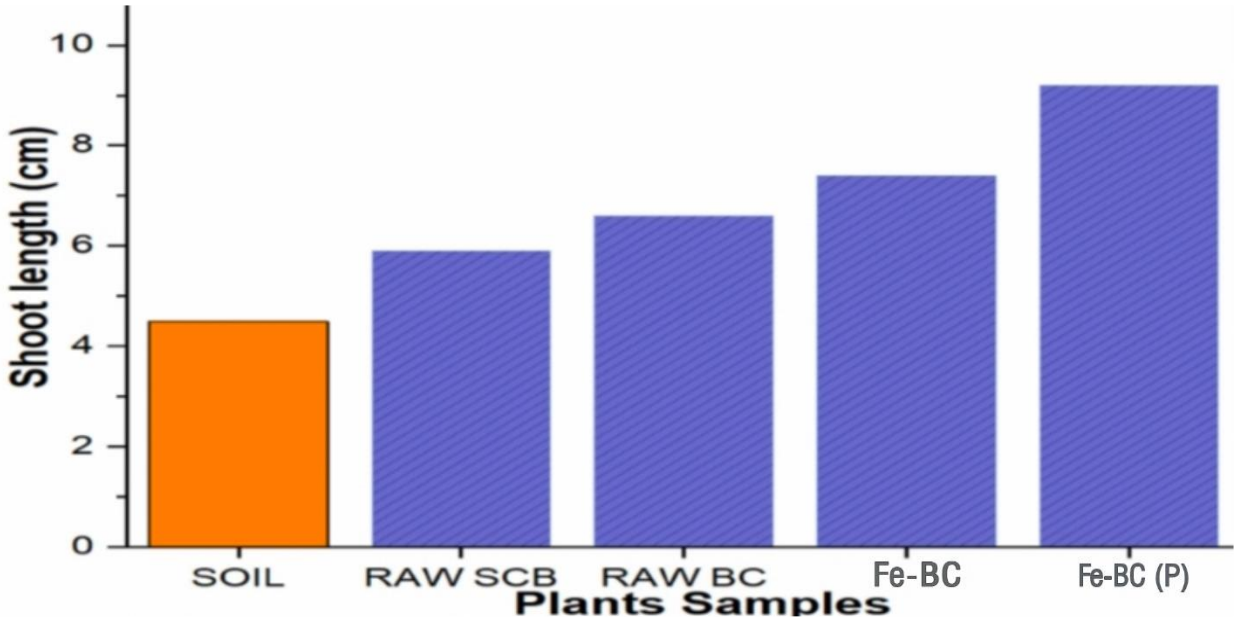

The pot test showed preliminary evidence that phosphate-loaded iron biochar may promote mustard plant growth, as indicated by improved shoot and root lengths compared with unmodified biochar and raw soil treatments. Nevertheless, as the experiment was scale-limited, the findings must be interpreted as an early growth response, rather than as fully agronomic validation.

During the data analysis phase, root and shoot length measurements from the pot test were analyzed to explore the impact of biochar addition on plant growth. To assess the significance of the results, we used statistical methods, including mean comparisons and t-tests. The analysis showed that adding biochar to the soil improved Mustard Plant growth. In particular, the length of

the roots and shoots rises with the activation of biochar with Fe. These results suggest that plant growth and development were positively affected by the activated biochar.

There are several reasons for the longer roots and shoots observed after Fe activation of biochar. The activated biochar may have improved nutrient availability and retention in the soil, providing essential components for plant growth. Additionally, it might have improved soil structure, enhancing aeration and water retention, which are essential for optimal plant growth. The results obtained are important, as they demonstrate how activated biochar can be used as a soil amendment to promote plant development. Activated biochar may enhance nutrient absorption, biomass production, and overall plant health by increasing root and shoot growth.

These results show that biochar-modified soil is suitable for plant cultivation and suggest that Fe-activated biochar can enhance its beneficial effects on plant growth. The use of iron-activated biochar as a sustainable, cost-effective soil additive has promising implications for farming practices and ecosystem restoration initiatives. It is important to acknowledge that further investigation and testing are needed to elucidate the underlying mechanisms and improve the use of Fe-activated biochar across various plant species and soil types. However, the present research adds to our understanding of biochar's potential as a useful approach in sustainable land management and agriculture.

COST AND BENEFIT ANALYSIS

5.1 The Process of Biochar Manufacturing

The manufacturing cost of biochar from sugarcane bagasse is approximately 2,200-2,500 PKR per tonne. The price range for sugarcane bagasse collection and transportation is 800-1,500 PKR. The pyrolysis procedure costs between 1,000 and 1,200 PKR, while the post-processing and storage expenses range from 400 to 800 PKR.

5.2 Regarding Rice Straw

In contrast, the overall cost per metric ton of producing biochar from rice straw has been estimated at 3,500 PKR. These calculations depict the expenditures associated with the collection and transportation of rice straw (1,600 PKR), the pyrolysis process (1,300 PKR), and the subsequent post-processing and storage (600 PKR).

According to the research findings, rice straw biochar demonstrates a maximum removal efficiency of 83%. Nonetheless, by optimizing all parameters, the maximum efficiency is anticipated to reach approximately 98.5%.

The value of the advantages gained from using biochar, as well as market demand and possible income from biochar sales, are additional considerations that must be included in a thorough cost-benefit analysis. Increased soil fertility, carbon sequestration, and reduced greenhouse gas emissions are among the possible outcomes of adopting such approaches.

A thorough review of overall expenses and potential earnings will help decision-makers in Pakistan determine whether or not biochar production from sugarcane bagasse and rice chaff is economically viable and profitable. This study aims to help people make better decisions by evaluating the practicality and sustainability of the biochar manufacturing method.

CONCLUSION

The findings of this study reveal that, after optimizing parameters such as pH and operating conditions, a remarkable removal efficiency of 80.25% was achieved under ambient conditions at pH 7. This emphasizes the potency of the functionalized biochar in eradicating a substantial portion of the targeted contaminants from water. Furthermore, using all optimal parameters, a maximum efficiency of 98.3% could be attained. This outcome demonstrates the tremendous potential of functionalized biochar when favorable conditions are met and applied. Additionally, the kinetics of the adsorption process can be better understood by considering the pseudo-second-order reaction model.

The results of this study indicate that the adsorption of contaminants onto iron-loaded biochar can be described by the Langmuir Isotherm model. Overall, the findings highlight functionalized biochar's potential as an environmentally feasible and sustainable method

for treating eutrophic water and recovering essential nutrients. This emphasizes the broader implications of the study, showcasing the promising capability of functionalized biochar in addressing the challenges associated with excessive nutrient levels in water bodies while potentially enabling the reuse or recycling of valuable extracted nutrients.

The results may differ from those in actual eutrophic waters with competing ions, organic matter, suspended particles, and fluctuating pH, as this study was conducted primarily in controlled laboratory settings. Acidic conditions achieved the highest removal efficiency, which would not be feasible for large-scale treatment without pH modification. Replicated trials, longer growth periods, soil nutrient analysis, and phosphate-release tests should be used to expand the preliminary pot test. Future research should use actual eutrophic lake water to evaluate regeneration, reuse, Fe leaching, cost, and performance.

REFERENCES

Ahmad, M., Rajapaksha, A. U., Lim, J. E., Zhang, M., Bolan, N., Mohan, D., Vithanage, M., Lee, S. S., & Ok, Y. S. (2014). Biochar as a sorbent for contaminant management in soil and water: A review. *Chemosphere*, *99*, 19–33. https://doi.org/10.1016/j.chemosphere.2013.10.071

Carpenter, S. R., Caraco, N. F., Correll, D. L., Howarth, R. W., Sharpley, A. N., & Smith, V. H. (1998). Nonpoint Pollution of Surface Waters with Phosphorus and Nitrogen. *Ecological Applications*, *8*, 559–568. https://doi.org/10.1890/1051-0761(1998)008[0559:NPOSWW]2.0.CO;2

Choi, Y. K., Jang, H. M., Kan, E., Wallace, A. R., & Sun, W. (2018). Adsorption of phosphate in water on a novel calcium hydroxide-coated dairy manure-derived biochar. *Environmental Engineering Research*, *24*(3), 434–442. https://doi.org/10.4491/eer.2018.296

Conley, D. J., Paerl, H. W., Howarth, R. W., Boesch, D. F., Seitzinger, S. P., Havens, K. E., Lancelot, C., & Likens, G. E. (2009). Controlling Eutrophication: Nitrogen and Phosphorus. *Science*, *323*(5917), 1014–1015. https://doi.org/10.1126/science.1167755

EPA. (2025, December 22). *Indicators: Phosphorus*. United States Environmental Protection Agency. https://www.epa.gov/national-aquatic-resource-surveys/indicators-phosphorus

Lehmann, J., & Joseph, S. (2015). *Biochar for Environmental Management: Science, Technology and Implementation* (2nd ed.). Routledge. https://doi.org/10.4324/9780203762264

Luo, D., Wang, L., Nan, H., Cao, Y., Wang, H., Kumar, T. V., & Wang, C. (2023). Phosphorus adsorption by functionalized biochar: a review. *Environmental Chemistry Letters*, *21*(1), 497–524. https://doi.org/10.1007/s10311-022-01519-5

Manyatshe, A., Cele, Z. E. D., Balogun, M. O., Nkambule, T. T. I., & Msagati, T. A. M. (2022). Chitosan modified sugarcane bagasse biochar for the adsorption of inorganic phosphate ions from aqueous solution. *Journal of Environmental Chemical Engineering*, *10*(5). https://doi.org/10.1016/j.jece.2022.108243

Palansooriya, K. N., Kim, S., Igalavithana, A. D., Hashimoto, Y., Choi, Y. E., Mukhopadhyay, R., Sarkar, B., & Ok, Y. S. (2021). Fe(III) loaded chitosan-biochar composite fibers for the removal of phosphate from water. *Journal of Hazardous Materials*, *415*. https://doi.org/10.1016/j.jhazmat.2021.125464

Rajapaksha, A. U., Chen, S. S., Tsang, D. C. W., Zhang, M., Vithanage, M., Mandal, S., Gao, B., Bolan, N. S., & Ok, Y. S. (2016). Engineered/designer biochar for contaminant removal/immobilization from soil and water: Potential and implication of biochar modification. *Chemosphere*, *148*, 276–291. https://doi.org/10.1016/j.chemosphere.2016.01.043

Smith, V. H., & Schindler, D. W. (2009). Eutrophication science: where do we go from here? *Trends in Ecology & Evolution*, *24*(4), 201–207. https://doi.org/10.1016/j.tree.2008.11.009

Vikrant, K., Kim, K. H., Ok, Y. S., Tsang, D. C. W., Tsang, Y. F., Giri, B. S., & Singh, R. S. (2018). Engineered/designer biochar for the removal of phosphate in water and wastewater. *Science of The Total Environment*, *616–617*, 1242–1260. https://doi.org/10.1016/j.scitotenv.2017.10.193

Yang, Q., Wang, X., Luo, W., Sun, J., Xu, Q., Chen, F., Zhao, J., Wang, S., Yao, F., Wang, D., Li, X., & Zeng, G. (2018). Effectiveness and mechanisms of phosphate adsorption on iron-modified biochars derived from waste activated sludge. *Bioresource Technology*, *247*, 537–544. https://doi.org/10.1016/j.biortech.2017.09.136

Yin, Q., Liu, M., Li, Y., Li, H., & Wen, Z. (2021). Computational study of phosphate adsorption on Mg/Ca modified biochar structure in aqueous solution. *Chemosphere*, *269*. https://doi.org/10.1016/j.chemosphere.2020.129374

Zhang, X., Liu, X., Zhang, Z., & Chen, Z. (2021). Removal of phosphate from aqueous solution by chitosan coated and lanthanum loaded biochar derived from urban dewatered sewage sludge: adsorption mechanism and application to lab-scale columns. *Water Science and Technology*, *84*(12), 3891–3906. https://doi.org/10.2166/wst.2021.485

Zhao, L., Cao, X., Zheng, W., Scott, J. W., Sharma, B. K., & Chen, X. (2016). Copyrolysis of biomass with phosphate fertilizers to improve biochar carbon retention, slow nutrient release, and stabilize heavy metals in soil. *ACS Sustainable Chemistry & Engineering*, *4*(3), 1630–1636. https://doi.org/10.1021/acssuschemeng.5b01570

Zheng, Y., Wang, B., Wester, A. E., Chen, J., He, F., Chen, H., & Gao, B. (2019). Reclaiming phosphorus from secondary treated municipal wastewater with engineered biochar. *Chemical Engineering Journal*, *362*, 460–468. https://doi.org/10.1016/j.cej.2019.01.036